OPTICAL BISTABILITY EFFECT IN DFB LASER WITH TWO SECTIONS

Nguyen Van Phu*, **Dinh Van Hoang**†, **Cao Long Van**#

* *Faculty of Physics, Vinh University*

† *Faculty of Physics, Hanoi National University*

\# *Institute of Physics, University of Zielona Góra*

Podgórna 50, 65-246 Zielona Góra, Poland

ABSTRACT. In this paper the optical bistability in DFB laser with two sections has been demonstrated. Influence of some dynamical laser parameters involved in the problem (as current intensity, saturation coefficient and gain values) on this effect has been considered.

1. Introduction

As known, the large number of DFB (distributed feedback) lasers used inside a transmitter makes the design and maintenance of such a light wave system expensive and impractical. The availability of semiconductor lasers which can be tuned over a wide spectral range would solve this problem. One of these is multi-(two or more) section DFB laser, considered theoretically and experimentally during 1980s [1]-[7], [13]-[18] and were used in commercial lightwave systems by 1990.

On the other hand, optical bistability effect, discovered since the 1970s in different optical systems with the possibility of its applications as an optical switch (or 'optical transistor'), an optical differential amplifier, optical limiter, optical clipper, optical discriminator, or an optical memory element, has given rise to a large number of different theoretical and experimental treatments. Because of many special advantages of utilizing semiconductors as optical bistable elements, the most efforts of researchers in the field of optical bistability have been focused on developing various semiconductor materials and devices [19].

In this paper we propose ones of theses devices: a DFB semiconductor laser with two sections. In Section II, starting from dynamical equations describing this laser we have received the exhibition of optical bistability effect in the stationary state limit. The influence of some dynamical laser parameters on this effect are demonstrated in Section III. Section IV contains conclusions.

Typeset by $\mathcal{A}\mathcal{M}\mathcal{S}$-TEX

2. System of rate equations—

The operating characteristics of semiconductor lasers are described by a set of rate equations that govern the interaction of photons and electrons inside the active region. A rigorous derivation of the rate equations generally starts from Maxwell's equations together with a quantum-mechanical approach for the induced polarization. A DFB laser with two sections is shown schematically in figure 1. Here, section A with injection current I_1 is an amplifying section, section B with injection current I_2 much smaller than I_1 takes a role as a saturable absorber section.

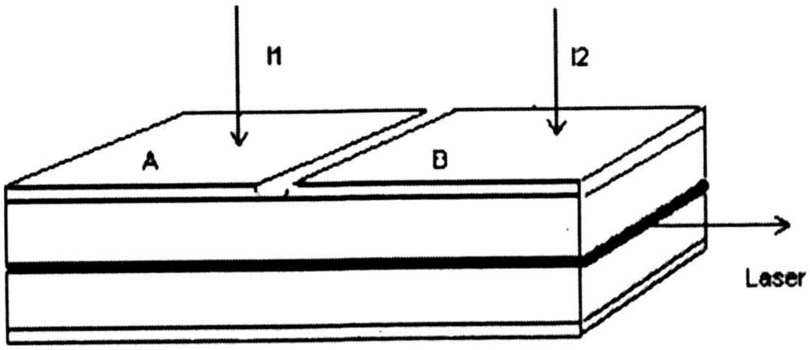

Fig.1. Schematic illustration of a DFB laser with two sections.

Then we have the following system of rate equations:

$$\frac{dN_1}{dt} = \frac{I_1}{eV_1} - \eta_1 \frac{c_0}{n_{eff}} g(\omega_0 - \omega_j) n_j - \gamma_1 N_1 \tag{1}$$

$$\frac{dN_2}{dt} = \frac{I_2}{eV_2} - \eta_2 \frac{c_0}{n_{eff}} g(\omega_0 - \omega_j) n_j - \gamma_2 N_2 \tag{2}$$

$$\frac{dn_j}{dt} = (\Gamma_1\eta_1 + \Gamma_2\eta_2) \frac{c_0}{n_{eff}} g(\omega_0 - \omega_j)(n_j + 1) - \gamma n_j + \beta\sqrt{P_\omega n_j} \tag{3}$$

Here V_1, V_2, N_1, N_2 are the volumes and carrier densities of sections A, B correspondingly; n_j is photon density; e, c_0 are electric charge of electron and velocity of light in vacuum; n_{eff} is the effective refraction index of material, supposed to be the same for two sections; η_i is the amplification coefficient, which depends on the carrier density in the form $\eta_i = \alpha_i N_i + \beta_i$, where α_i, β_i are material gain coefficients $(i = 1, 2)$; γ_1, γ_2 are relaxation coefficients of carrier densities given in the form [8]

$$\gamma_1 = \frac{B_0 N_1}{1 - B_1 N_1}, \quad \gamma_2 = \xi \frac{B_0 N_2}{1 - B_2 N_2},$$

with B_0, B_1, B_2 are material coefficients, ξ is saturation coefficient indicating the different relaxations of carrier densities between two sections; Γ_1, Γ_2 are confinement factors or Peterman coefficients in sections A and B; γ is coefficient which describes the photon loss in section A, B and mirrors; Function $g(\omega_0 - \omega_j)$ describes the broadening of spectral laser line which is given in the form of Lorentzian:

$$g(\omega_0 - \omega_j) = \frac{1}{1 + \left(\frac{2\Delta_j}{\Gamma}\right)^2}$$

with Γ is the width of the gain line; $\Delta_j = \omega_0 - \omega_j$ is detuning factor; ω_0, ω_j are circular frequencies in the center of the gain line and of j^{th} mode. The unity in factor $(n_j + 1)$ indicates the presence of spontaneous emission in laser operation and the last term $\beta\sqrt{n_j P_\omega}$ deals with the interaction of signal and laser radiation. The interaction coefficient β is usually taken to be unity ($\beta = 1s^{-1}$ [7]-[8]).

In the stationary regime, we put all time derivatives in (1), (2), (3) to zero and obtain:

$$0 = \frac{I_1}{eV_1} - \eta_1 \frac{c_0}{n_{eff}} g(\omega_0 - \omega_j) n_j - \gamma_1 N_1, \tag{4}$$

$$0 = \frac{I_2}{eV_2} - \eta_2 \frac{c_0}{n_{eff}} g(\omega_0 - \omega_j) n_j - \gamma_2 N_2, \tag{5}$$

$$0 = (\Gamma_1\eta_1 + \Gamma_2\eta_2) \frac{c_0}{n_{eff}} g(\omega_0 - \omega_j)(n_j + 1) - \gamma n_j + \beta\sqrt{P_\omega n_j}. \tag{6}$$

We suppose also that $\beta_i = 0$, which is usually valid for the most of semiconductor lasers used in practice (e.g. InGaAsP, see [7], [8]) and we also suppose to ignore the presence of spontaneous emission. It follows from (4), (5), (6) that

$$An_j^{7/2} - En_j^{5/2} + Cn_j^{3/2} - Dn_j^{1/2} + \beta\sqrt{P_\omega} G n_j - \beta\sqrt{P_\omega} Q n_j^2 - \beta\sqrt{P_\omega} = 0, \tag{7}$$

where the coefficients A, E, C, D, G, Q are given by:

$$A = \frac{\Gamma_1\alpha_1^3\alpha_2\nu^4 g^4 eV_1 B_2}{4\xi B_0^2 T_{11}} + \frac{\Gamma_2\alpha_1\alpha_2^3\nu^4 g^4 eV_2 B_1}{4\xi B_0^2 T_{22}},$$

$$E = \frac{\Gamma_1\alpha_1^3\nu^3 g^3 eV_1}{4B_0 T_{11}} + \frac{\Gamma_2\alpha_2^3\nu^3 g^3 eV_2}{4\xi B_0 T_{22}} + \frac{\Gamma_1\alpha_1^2\alpha_2\nu^3 g^3 I_1 B_1 B_2}{2\xi B_0^2 T_{11}} + \frac{\Gamma_2\alpha_1\alpha_2^2\nu^3 g^3 I_2 B_1 B_2}{2\xi B_0^2 T_{22}}$$
$$+ \frac{\Gamma_1\alpha_1^2\alpha_2\nu^3 g^3 B_2 + \Gamma_2\alpha_1\alpha_2^2\nu^3 g^3 B_1 - 2\gamma\alpha_1\alpha_2\nu^2 g^2 B_1 B_2}{2\xi B_0^2},$$

$$C = \frac{\Gamma_1\alpha_1^2 g^2\nu^2 I_1 B_1}{2B_0 T_{11}} + \frac{\Gamma_2\alpha_2^2\nu^2 g^2 I_2 B_2}{2\xi B_0 T_{22}} + \frac{\Gamma_1\alpha_1^2\nu^2 g^2\xi + \Gamma_2\alpha_2^2\nu^2 g^2}{2\xi B_0}$$
$$+ \frac{\Gamma_1\alpha_1\alpha_2\nu^2 g^2 B_2}{2\xi B_0^2 eV_1} T_{11} + \frac{\Gamma_2\alpha_1\alpha_2\nu^2 g^2 B_1}{2\xi B_0^2 eV_2} T_{22}$$
$$- \frac{\Gamma_1\alpha_1\alpha_2\nu^2 g^2 I_1 B_1 B_2}{2\xi B_0^2 eV_1} - \frac{\Gamma_2\alpha_1\alpha_2\nu^2 g^2 I_2 B_1 B_2}{2\xi B_0^2 eV_2} - \frac{\gamma\alpha_1\nu g B_1\xi + \gamma\alpha_2\nu g B_2}{\xi B_0},$$

$$D = \frac{\Gamma_1\alpha_1\nu g}{2B_0 eV_1} T_{11} + \frac{\Gamma_2\alpha_2\nu g}{2\xi B_0 eV_2} T_{22} - \frac{\Gamma_1\alpha_1\nu g I_1 B_1}{2B_0 eV_1} - \frac{\Gamma_2\alpha_2\nu g I_2 B_2}{2\xi B_0 eV_2} - \gamma,$$

$$G = \frac{\alpha_1 \nu g B_1}{B_0} + \frac{\alpha_2 \nu g B_2}{\xi B_0}; \; Q = \frac{\alpha_1 \alpha_2 \nu^2 g^2 B_1 B_2}{\xi B_0^2};$$
$$\nu = \frac{c_0}{n_{eff}}; \; g = g(\omega_0 - \omega_j),$$
$$T_{11} = \sqrt{4 I_1 B_0 e V_1 + I_1^2 B_1^2}; \; T_{22} = \sqrt{4 \xi I_2 B_0 e V_2 + I_2^2 B_2^2}.$$

When the external optical signal disappears ($P_\omega = 0$), we obtain from (7)

$$A n_j^3 - E n_j^2 + C n_j - D = 0. \tag{8}$$

For the most of semiconductor lasers used in practice we have also [7] $V_1 = V_2 = V$, $B_1 = B_2 = B$, $\alpha_1 = \alpha_2 = \alpha$. We consider for simplicity the resonance case in which the generating mode frequency coincides with ω_0, then we have

$$g(\omega_0 - \omega_j) = 1.$$

and obtain finally:

$$n_j^3 - \mathcal{H} n_j^2 + \mathcal{L} n_j - \mathcal{M} = 0, \tag{9}$$

where:

$$\mathcal{H} = \left[\frac{B_0}{B}(\xi \Gamma_1 T_{22} + \Gamma_2 T_{11}) + \frac{2B}{eV}(\Gamma_1 I_1 T_{22} + \Gamma_2 T_2 T_{11}) + \frac{2 T_{11} T_{22}}{\alpha \nu e V}(\Gamma_1 \alpha \nu + \Gamma_2 \alpha \nu - 2\gamma B) \right] / \mathcal{T}$$
$$\mathcal{L} = \left[\frac{2}{\alpha \nu e V} B_0 (\xi \Gamma_1 I_1 T_{22} + \Gamma_2 I_2 T_{11}) + \frac{B_0 T_{11} T_{22}}{B}(\xi \Gamma_1 + \Gamma_2) + \frac{T_{11} T_{22}}{eV}(\Gamma_1 T_{11} + \Gamma_2 T_{22}) \right] / \mathcal{T}$$
$$- \left[\frac{B T_{11} T_{22}}{eV}(I_1 \Gamma_1 + I_2 \Gamma_2) + \frac{2\gamma B_0 T_{11} T_{22}}{\alpha \nu}(\xi I_1 + 1) \right] / \mathcal{T}$$
$$\mathcal{M} = \frac{2 B_0 T_{11} T_{22}}{\alpha^2 \nu^2 e V} \left[\frac{1}{BeV}(\xi \Gamma_1 T_{11} + \Gamma_2 T_{22}) - \frac{1}{eV}(\xi I_1 \Gamma_1 + I_2 \Gamma_2) - \frac{\xi \gamma B_0}{\alpha \nu B} \right] / \mathcal{T}$$
$$\mathcal{T} = \alpha \nu (\Gamma_1 T_{22} + \Gamma_2 T_{11}),$$

The Eq. (9) represents the catastrophe manifold of the Riemann-Hugoniot (or 'cusp') catastrophe A_3 in the Mather-Thom classification [20]. This catastrophe is given by the following potential function $V(x; a, b)$:

$$V(x; a, b) = \frac{1}{4} x^4 + \frac{1}{2} a x^2 + b x. \tag{10}$$

The physical system described by this potential function has evolution generated by variations in the control parameters $a = \mathcal{L} - \mathcal{H}^2/3, b = \mathcal{H}\mathcal{L}/3 - \mathcal{M} - 2\mathcal{H}^3/27$. The system, in accordance with the general principle of minimization of potential energy, will tend to dwell on the catastrophe surface M_3 given by

$$M_3 = \{(x, a, b) : x^3 + ax + b = 0\}.$$

The set of degenerate critical points Σ_3, defined by the condition of having multiple roots by the polynomial $w(x) = x^3 + ax + b$, is expressed by

$$\Sigma_3 = \left\{(x, a, b) : x^3 + ax + b = 0, 3x^2 + a = 0\right\}. \tag{11}$$

The x variable may be eliminated from the system of equations defining the set Σ_3. Then we obtain the bifurcation set B_3 given by:

$$B_3 = \{(a, b) : 4a^3 + 27b^2 = 0\}.$$

This set determines the parameters range involved in the problem for which the bistablity effect occurs. The left side of (9) is an universal unfolding of the function $f(n_j) = n_j^3$ which is structurally stable: the small change of the control parameters (physical parameters involved in the problem) do not change the form of the hysteresis curves as we will see in the next Section.

3. Influence of some dynamical parameters on optical bistability effect

3.1. The appearance of optical bistability effect

We can now solve numerically the equations (7), (8). The values of the parameters involved in the problem are taken from the experimental data for a concrete semiconductor laser on InGaAsP given by Kinoshita [7] and Yong-Zhen Huang [8]: $c_0 = 3.10^{10} cm.s^{-1}$; $e = 1,6.10^{-19} C$; $V_1 = 84.10^{-12} cm^3$; $V_2 = 84.10^{-12} cm^3$; $B_0 = 10^{-10} cm^3.s^{-1}$; $B_1 = 5.10^{-19} cm^3$; $B_2 = 5.10^{-19} cm^3$; $n_{eff} = 3.4$; $\alpha_1 = 4.10^{-16} cm^2$; $\alpha_2 = 4.10^{-16} cm^2$; $\xi = 0.1$; $\Gamma_1 = 0.5$; $\Gamma_2 = 0.2$; $\gamma = 1,71.10^{12} s^{-1}$; $\beta_i = 0$; $\beta = 1 s^{-1}$; $P_\omega = 10^{22} cm^{-3}$.

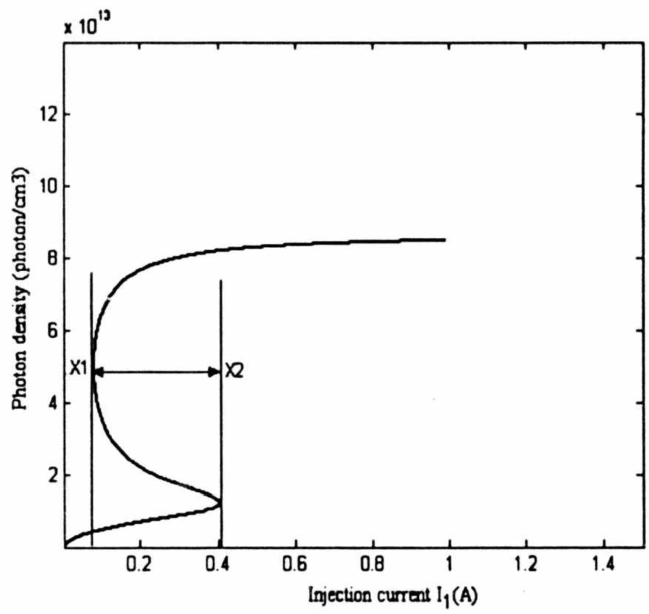

Fig.2. Hysteresis curve of optical bistability effect in DFB laser with two sections.

In the MATLAB language, we have received a hysteresis curve of optical bistability effect shown in Fig. 2. Here injection current I_1 is control parameter and distance X1X2 indicates the width of bistability (BSW).

3.2. The change of the injection current I_2

It follows from Fig. 3, that when I_2 increases, the bistability width (BSW) increases too. For clearness we take three values of I_2 : $2 \times 10^{-5}A, 2.5 \times 10^{-5}A, 2.8 \times 10^{-5}A$. The corresponding curves are presented in Fig. 3: The dotted line corresponds to the value of $I_2 = 2 \times 10^{-5}A$, the dashed and solid lines correspond to the values of $I_2 = 2.5 \times 10^{-5}A$ and $I_2 = 2.8 \times 10^{-5}A$. The results are given in the Table I.

Table I

$I_2(A)$	2×10^{-5}	2.5×10^{-5}	2.8×10^{-5}
$BSW(A)$	0.1543	0.4423	1.3486

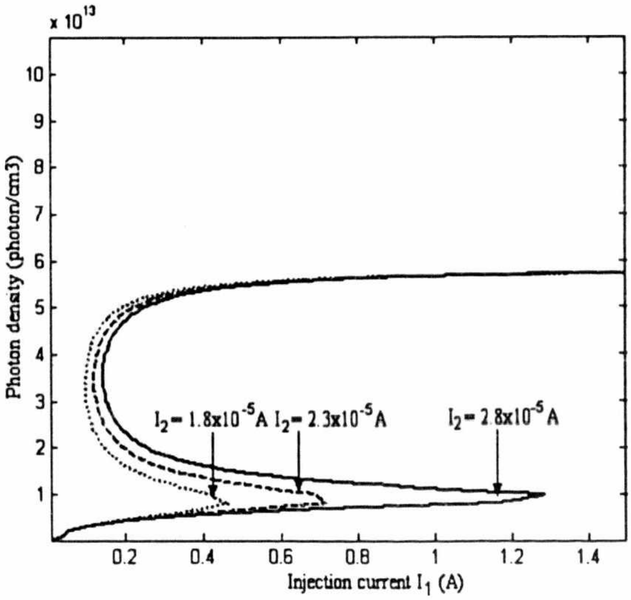

Fig. 3. Influence of injection current I_2 on hysteresis curves of optical bistability effect. Other values of I_2 are $I_2 = 2 \times 10^{-5}A, I_2 = 2.5 \times 10^{-5}A, I_2 = 2.8 \times 10^{-5}A$.

3.3. Influence of the saturation coefficient ξ

Choosing three values of ξ we also obtain the hysteresis curves and optical bistabilty effect is demonstrated in Fig. 4. When ξ rises the BSW diminishes. The results are given in Table II.

Table II

ξ	0.1	0.15	0.2
$BSW(A)$	0.4354	0.2194	0.1343

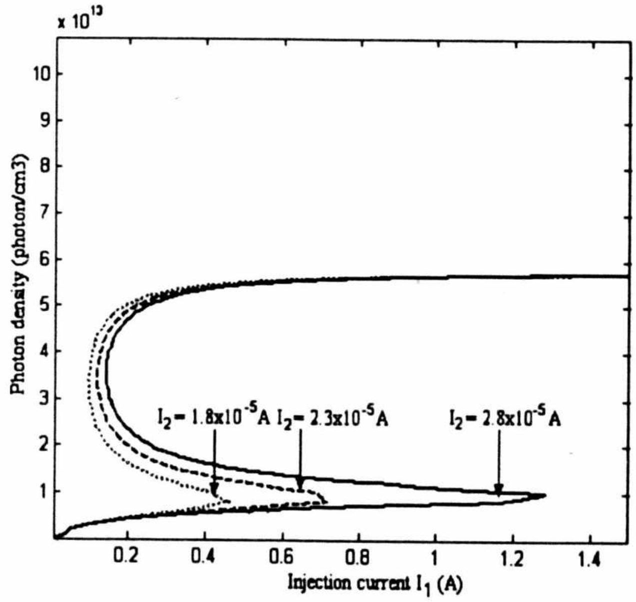

Fig. 4. Influence of saturation coefficient ξ on BSW of hysteresis curves

3.4. Influence of the gain value α

In this case the curves of optical bistability are presented in Fig. 5. From this Fig., we see that when the gain value α increases the BSW increases too. The numerical results are given in Table III.

Table III

$\alpha(cm^2)$	3×10^{-16}	4×10^{-16}	5×10^{-16}
$BSW(A)$	0.4354	0.6857	1.1211

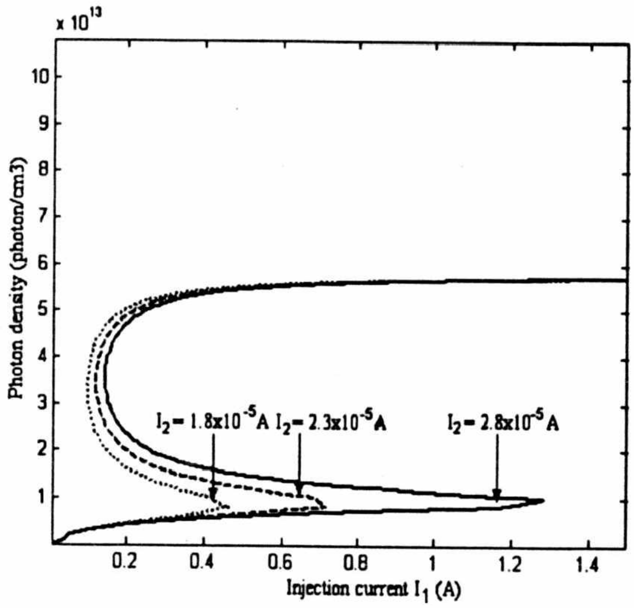

Fig. 5. Influence of gain values α on hysteresis curves of optical bistability effect.

5. Conclusions

From above obtained results we derive the following conclusions:

1. Optical bistability effect appeared like in the case of lasers containing saturable absorber (LSA) [16]. Here, the decisive condition for having hysteresis curves of OB effect is the current I_2 in section B must be much smaller than current I_1 in section A.

2. Laser parameters as gain, saturation coefficients, etc ... will be control parameters for hysteresis curves. The change of dynamical parameters involved in the problem clearly influences on characteristics of optical bistability effect as the bistability width or the optical bistability height. Determination of the values of these parameters, which give the large bistability width for DFB laser is very important from experimental and practical point of view.

In fact, the change values of laser parameters as gain, saturation coefficients, etc... can be realized by changing proportion of x or y in structure $In_{1-x}Ga_xAs_yP_{1-y}$ of material.

5. References

1. Dinh Van Hoang et al., *Modern problems in Optics and Spectroscopy*, II, 406 (2000).
2. G. Morthier and P. Vankwikelberge, *Handbook of Distributed Feedback Laser Diodes*, Artech House, Norwood, MA 1999, p. 1792.
3. A. Lugiato, L. M. Narducci, *Phys. Rev. A* **32**, 1576 (1985).
4. D. Dangoisse et al., *Phys. Rev. A* **42**, (1990) 1551.
5. H. Wenzel et al., *IEEE J. Quantum Elec.* **32**, 69 (1996).
6. B. Sartorius et al., *IEEE J. Quantum Elec.* **33**, 211 (1997).
7. J. Kinoshita, *IEEE J. Quantum Elec.* **30**, 928 (1990).
8. Yong-Zhen Huang,*IEEE Photonics Tech. Lett.* **7**, 977 (1995).
9. H. Onaka et al., in: *Optical Fiber Communication (OFC'96).* Post deadline papers, Part B, San Jose, 25 Feb.-1 Mar., pp. PD 19-1/5.
10. G. P. Makino et al., in: *Optical Fiber Communication (OFC'96).* Technical Digest, Vol. 2, San Jose, 25 Feb.-1 Mar., pp. PD 298-142.
11. I. Jiondot and I. L. Beylat, *Electron Lett.* **29**, 604 (1993).
12. S. M. Sze, *Physics of semiconductor devices*, 2nd ed., Wiley, New York 1981.
13. K. Seeger, *Semiconductor Physics*, Springer-Verlag, Berlin 1985.
14. M. Asada et al., *IEEE J. Quantum Elec.* **17**, 947 (1981).
15. K. Iga and S. Kinoshita, *Process technology for semiconductor laser*, Springer series in materials science, New York 1996.
16. P.Q. Bao, D.V. Hoang and Luc, *J. of Russian Laser Research*, Kluwer Academic/Plen Publishers, Vol. 20, No. 4, 297 (1999).
17. G. P. Agrawal, *Fiber-Optic Communication Systems*, 3rd ed., John Wiley & Sons, inc., New York 2002.
18. M. Ohstu, *Frequency Control of Semiconductor Lasers*, Wiley, New York 1996.
19. G.S. He, S.H. Liu, *Physics of nonlinear optics*, World Scientific Publishing Co. Pte. Ltd, Singapore 1999, Chapter 12.
20. G. Gilmore, *Catastrophe Theory for Scientists and Engineers*, New York 1981.